

LLM-VA: Resolving the Jailbreak-Overrefusal Trade-off via Vector Alignment

Anonymous ACL submission

Abstract

Safety-aligned LLMs suffer from two failure modes: jailbreak (responding to harmful inputs) and over-refusal (declining benign queries). Existing vector steering methods adjust the magnitude of answer vectors, but this creates a fundamental trade-off—reducing jailbreak increases over-refusal and vice versa. We identify the root cause: LLMs encode the decision to respond (answer vector v_a) and the judgment of input safety (benign vector v_b) as nearly orthogonal directions, treating them as independent processes. We propose LLM-VA, which aligns v_a with v_b through closed-form weight updates, making the model’s willingness to respond causally dependent on its safety assessment—without fine-tuning or architectural changes. Our method identifies vectors at each layer using SVMs, selects safety-relevant layers, and iteratively aligns vectors via minimum-norm weight modifications. Experiments on 12 LLMs demonstrate that LLM-VA achieves 11.45% higher F1 than the best baseline while preserving 95.92% utility, and automatically adapts to each model’s safety bias without manual tuning. Code and models are available at <https://anonymous.4open.science/w/LLM-VA-Web-A6C4/>.

1 Introduction

Large language models (LLMs) have achieved remarkable capabilities across diverse NLP tasks (OpenAI, 2024; Team, 2025; AI@Meta, 2024), yet safety alignment remains challenging. Safety-aligned LLMs exhibit two failure modes: *jailbreak*, where the model responds to toxic inputs (i.e., queries designed to elicit harmful, unethical, or unsafe responses) (Yi et al., 2024; Zou et al., 2023b; Yuan et al., 2025), and *over-refusal*, where the model unnecessarily declines benign queries (Röttger et al., 2024; Zhang et al., 2025a; Cui et al., 2025). This dual failure mode significantly limits the deployment of LLMs in safety-

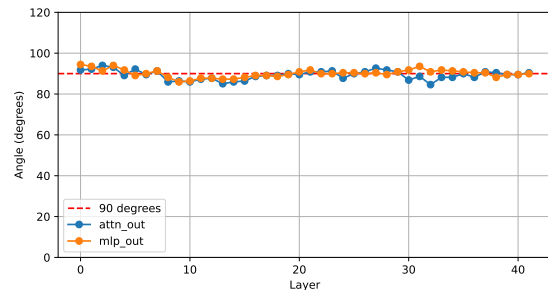


Figure 1: The angles between answer vectors (v_a) and benign vectors (v_b) are approximately 90° across layers in gemma-2-9b-it, indicating near-orthogonality between response decisions and safety assessments.

critical applications, where both reliability and usability are essential. Among approaches to address these issues, vector steering (Zou et al., 2023a; Arditì et al., 2024; Sheng et al., 2025) has gained attention for its efficiency—it manipulates specific directions in the model’s latent space without costly retraining, using only simple answer/refuse labels rather than fine-grained annotations.

However, existing vector steering methods only adjust the *magnitude* of the answer vector, creating a fundamental trade-off: reducing magnitude suppresses jailbreak but increases over-refusal, while amplifying it has the opposite effect (Arditì et al., 2024; Sheng et al., 2025). Recent methods like SCANS (Cao et al., 2025) and CAST (Lee et al., 2024) incorporate input toxicity but require architectural modifications and treat both failure modes as separate objectives (see Table 1). This magnitude-based paradigm cannot fundamentally resolve the trade-off.

We identify the root cause of this trade-off: existing methods control *output behavior* (answer vs. refuse) without considering *input characteristics* (benign vs. toxic). To investigate, we extract two vectors at each layer: the *answer vector* (v_a), indicating whether the model will respond, and the

benign vector (v_b), indicating whether the input is safe. As shown in Figure 1, these vectors are nearly orthogonal ($\sim 90^\circ$) across layers,¹ revealing that LLMs treat response decisions and safety assessments as *independent* processes. This explains both failure modes: the model may answer toxic inputs (jailbreak) or refuse benign ones (over-refusal) because its willingness to respond is decoupled from its judgment of input safety.

Based on this observation, we propose Large Language Model Vector Alignment (LLM-VA). By aligning these vectors, we make the model’s willingness to respond *causally dependent* on its safety assessment (Zou et al., 2023a), rather than treating them as independent decisions. Crucially, LLM-VA achieves this through closed-form weight updates—requiring no gradient-based optimization, fine-tuning, or architectural changes. Our method involves three steps:

- **Vector identification via SVMs:** Train SVMs at each layer to find hyperplanes separating benign/toxic and answer/refuse samples, yielding both v_b and v_a .
- **Layer selection:** Identify layers most relevant to safety decisions based on their contribution to final output and SVM classification accuracy.
- **Vector alignment:** Adjust layer weights to align v_a with v_b , ensuring benign inputs activate the “answer” direction while toxic inputs do not.

Extensive experiments on 12 LLMs demonstrate that LLM-VA achieves 11.45% higher F1 scores (effectiveness on resolving trade-off) than the best baseline (AlphaSteer) (Sheng et al., 2025) with only 4.08% model utility drop, indicating that LLM-VA effectively resolves the jailbreak-overrefusal trade-off while preserving general capabilities. In summary, our contributions are:

- We propose LLM-VA, which, to the best of our knowledge, is the first vector steering method that simultaneously addresses both jailbreak and over-refusal by aligning answer vectors with benign vectors through closed-form weight updates—requiring no gradient-based fine-tuning or architectural changes.
- We demonstrate on 12 LLMs from 5 model families that LLM-VA achieves state-of-the-art safety alignment, and show that it automatically adapts

to each model’s safety bias—prioritizing jailbreak reduction for vulnerable models and over-refusal reduction for overly conservative ones—without manual tuning.

- We release our code and safety-enhanced weights for 12 LLMs.²

2 Related Work

Safety Alignment and the Jailbreak-Overrefusal Trade-off Traditional safety alignment methods—RLHF (Christiano et al., 2017; Stiennon et al., 2020), adversarial training (Xhonneux et al., 2024; Liu et al., 2024a), and rule-based filtering (Zhang et al., 2025b)—require substantial computational resources or lack scalability. Vector steering (Zou et al., 2023a; Arditi et al., 2024) emerged as an efficient alternative, manipulating latent-space directions without retraining. However, these methods create a fundamental trade-off: reducing the answer vector’s magnitude suppresses jailbreak but increases over-refusal, while amplifying it has the opposite effect (Arditi et al., 2024; Sheng et al., 2025). This trade-off remains the central unsolved problem in efficient safety alignment.

Vector Steering Methods VectorSteer (Zou et al., 2023a) first identified answer vectors for controlling model outputs through magnitude adjustment. AlphaSteer (Sheng et al., 2025) introduced null-space projection to preserve utility during steering, but remains magnitude-based and thus inherits the trade-off. SCANS (Cao et al., 2025) and CAST (Lee et al., 2024) incorporate input toxicity information, representing progress toward input-aware steering. However, both require architectural modifications (hook layers) and still treat jailbreak and over-refusal as separate objectives to be balanced via hyperparameters. Table 1 summarizes these differences: LLM-VA is the only approach that addresses both failure modes without finetuning or architectural changes.

Internal Representations in LLMs Mechanistic interpretability research reveals that LLMs encode concepts as linear directions in their hidden states (Geva et al., 2021; Elhage et al., 2022; Zou et al., 2023a). Building on this foundation, we discover that answer vectors (v_a) and benign vectors

¹Results for other LLMs are similar; see Appendix A.

²Due to anonymity requirements, we release only Llama3.1-8B-Instruct weights during review. Full weights available at <https://figshare.com/s/f2aa365c87a80097a436>.

Table 1: Comparison of LLM-VA with other methods on safety alignment and utility preservation.

Method	w/o Finetuning	w/o Model Structure Modification	Over-refusal Mitigation	Jailbreak Mitigation
LLM-VA	✓	✓	✓	✓
Finetuning	✗	✓	✓	✓
VectorSteer	✓	✗	✗	✓
AlphaSteer	✓	✗	✗	✓
CAST	✓	✗	✓	✓
SCANS	✓	✗	✓	✓

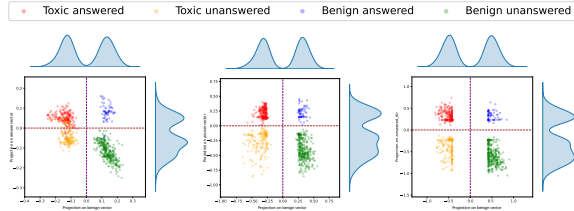


Figure 2: The distributions of the projections onto the benign, answer vectors at different layers of Llama-3.1-8B-Instruct. The left, middle, right figures correspond to the 4th, 16th, and 28th MLP layers, respectively.

(v_b) are nearly orthogonal across layers, explaining why magnitude-based methods cannot resolve the trade-off—they control output behavior independently of input safety. LLM-VA addresses this by aligning these vectors, making the answer decision causally dependent on the safety assessment.

3 Preliminary Analysis

To motivate our approach, we analyze how LLMs internally represent two distinct decisions: (1) whether to answer or refuse a query, and (2) whether the input is benign or toxic.³ Following Zou et al. (2023a), we extract the answer vector v_a and benign vector v_b at each layer on 128 randomly sampled toxic inputs from S-Eval (Yuan et al., 2025) and 128 benign inputs from ORFuzzSet (Zhang et al., 2025a).⁴ We project layer outputs onto these vectors and visualize the distributions in Figure 2. Three key observations emerge:

- Obs 1: LLMs encode both decisions internally.** Projections onto v_b cleanly separate benign from toxic inputs, while projections onto v_a separate answered from refused samples—both with decision boundaries near zero.
- Obs 2: Later layers are more discriminative.** Separation quality improves in deeper layers

³We define “answer” as providing a direct response and “refuse” as declining to respond.

⁴We illustrate with Llama-3.1-8B-Instruct; results are consistent across models.

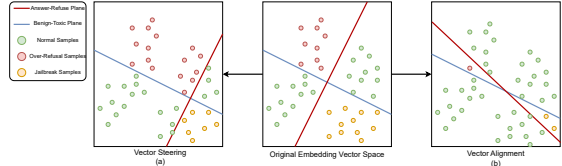


Figure 3: Unlike existing methods that only adjust the magnitude of v_a (trading off jailbreak vs. over-refusal), LLM-VA aligns v_a with v_b to address both issues.

(compare layers 4, 16, and 28 in Figure 2), indicating that later layers are more critical for safety-related decisions.

- Obs 3: The two decisions are misaligned.** Some toxic inputs project positively onto v_a , while some benign inputs project negatively. This misalignment directly causes jailbreak and over-refusal failures.

Combined with the near-orthogonality between v_a and v_b (Figure 1), these observations reveal that LLMs treat response decisions and safety assessments as *independent* processes. We hypothesize that *aligning* v_a with v_b —making the model’s willingness to answer depend on its safety judgment—will reduce both failure modes.

Why vector alignment, not magnitude adjustment? Existing vector steering methods (Sheng et al., 2025; Cao et al., 2025; Ray and Bhalani, 2024) only adjust the magnitude of v_a : reducing it decreases jailbreak risk but increases over-refusal, while increasing it has the opposite effect (Figure 3a). In contrast, LLM-VA aligns v_a with v_b (Figure 3b), making the answer decision depend on input safety rather than treating them independently.

Optimization Objective We formalize this goal as maximizing correct response behavior:

$$\max_{\theta} \mathbb{E}_x [\mathbb{I}(y=\text{benign}) \cdot \mathbb{I}(f_{\theta}(x)=\text{answer}) + \mathbb{I}(y=\text{toxic}) \cdot \mathbb{I}(f_{\theta}(x)=\text{refuse})] \quad (1)$$

where x is an input, $y \in \{\text{benign}, \text{toxic}\}$ its ground-truth label, and $f_{\theta}(x) \in \{\text{answer}, \text{refuse}\}$ the model’s response. By aligning v_a with v_b , projections onto v_a become correlated with input benignness, optimizing this objective. The following sections detail how LLM-VA achieves this.

4 Methodology

Building on our observation that LLMs encode answer decisions (v_a) and safety assessments

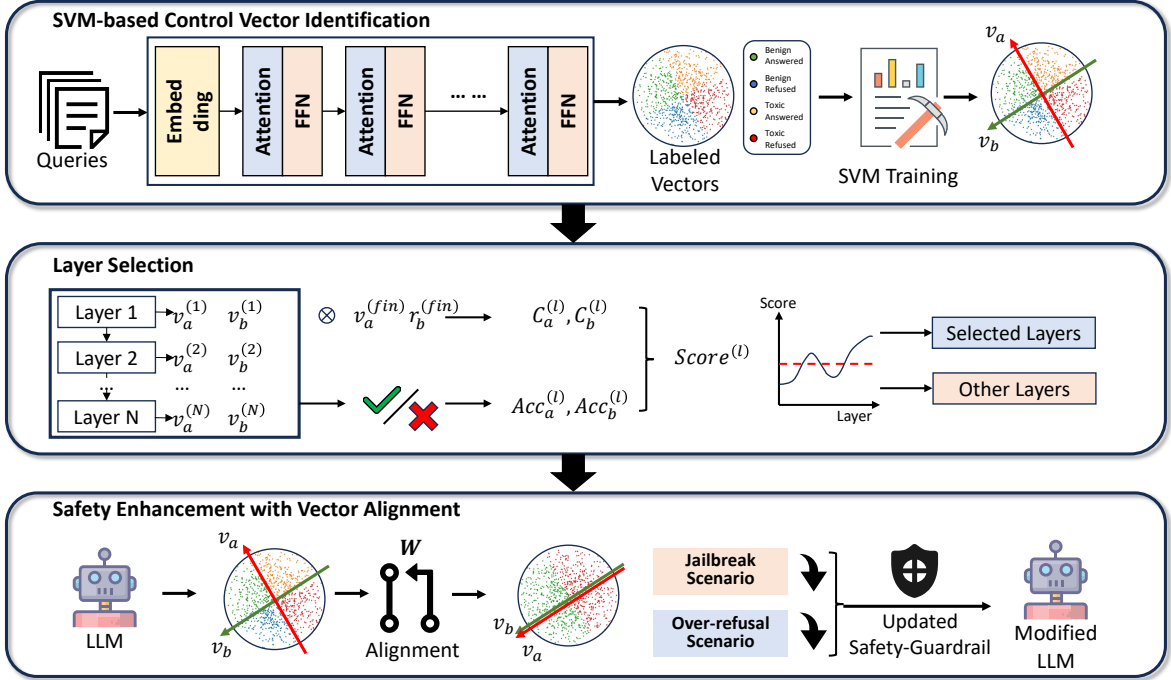


Figure 4: The framework of LLM-VA.

(v_b) as nearly orthogonal directions, we present LLM-VA. Our key insight is that by aligning these vectors through closed-form weight updates—requiring no gradient-based fine-tuning or architectural changes—we can make the model’s willingness to answer causally dependent on its safety judgment. As illustrated in Figure 4, LLM-VA mainly consists of three steps: (1) identifying v_a and v_b at each layer via SVMs (Section 4.1), (2) selecting layers most relevant to safety decisions (Section 4.2), and (3) deriving weight update process that aligns these vectors (Section 4.3).

4.1 SVM-based Control Vector Identification

To align vectors at each layer, we must first identify them. Prior work (Zou et al., 2023a; Sheng et al., 2025; Cao et al., 2025) extracts the answer vector from the residual flow at the final layer. However, since the residual flow aggregates contributions from all preceding layers, modifying individual layer weights cannot directly control the final-layer vector. To enable layer-wise weight modification, we instead extract vectors from each layer’s output.

At each layer, we train two linear SVMs to find hyperplanes separating (1) benign vs. toxic inputs, and (2) answered vs. refused samples. We use SVMs because they provide interpretable linear decision boundaries: the normal vector of the maximum-margin hyperplane directly yields the

control vector, and the margin maximization ensures robustness. The SVMs minimize (Cortes and Vapnik, 1995):

$$\begin{aligned} & \min_{w_{svm}, \zeta} \|w_{svm}\|_2^2 + C \sum_{i \in \mathcal{D}} \zeta_i, \\ & \text{s.t. } y_i(w_{svm} \cdot o_i^{(l)}) \geq 1 - \zeta_i, \forall i \in \mathcal{D} \end{aligned} \quad (2)$$

where $o_i^{(l)}$ is the output of layer l for input i , $y_i \in \{-1, 1\}$ is the label (+1 for benign/answer, and -1 for toxic/refuse), $C > 0$ is a regularization parameter, and $\zeta_i \geq 0$ are slack variables. We omit the bias term b_{svm} because our empirical analysis shows that decision hyperplanes pass through the origin. This simplifies the subsequent alignment formulation and implementation.

The unit normal vectors of these hyperplanes yield the control vectors:

$$v_b^{(l)} = w_b^{(l)} / \|w_b^{(l)}\| \quad (3)$$

$$v_a^{(l)} = w_a^{(l)} / \|w_a^{(l)}\| \quad (4)$$

where $w_b^{(l)}$ and $w_a^{(l)}$ are the SVM weight vectors for benign/toxic and answer/refuse classification at layer l , respectively.

4.2 Layer Selection

Not all layers contribute equally to safety decisions (Geva et al., 2021). Modifying irrelevant

224
225
226
227
228
229
230
231
232
233
234
235

236

252
253
254
255
256
257
258
259
260
261
262
263
264
265
266

267

268

269

270

271

272

273

274

275 layers wastes capacity and may harm utility, so we
 276 select layers that are both *influential* (their vectors
 277 align with the decisions of final residual stream)
 278 and *accurate* (their SVMs reliably distinguish be-
 279 nign/toxic or answer/refuse).⁵

280 **Influence on final decision.** Following prior
 281 work showing that the residual stream determines
 282 final outputs (Zou et al., 2023a; Sheng et al., 2025),
 283 we measure how well each layer’s vectors align
 284 with the vectors of final residual stream:

$$285 \quad C_a^{(l)} = v_a^{(fin)} \cdot v_a^{(l)}, \quad C_b^{(l)} = v_b^{(fin)} \cdot v_b^{(l)} \quad (5)$$

286 High $C^{(l)}$ indicates that modifying layer l ’s vector
 287 direction will propagate to the final decision.

288 **Classification accuracy.** We also require that the
 289 layer’s SVMs accurately separate the two classes.
 290 Let $\text{Acc}_a^{(l)}$ and $\text{Acc}_b^{(l)}$ denote validation accuracies
 291 for the answer and benign classifiers at layer l .

292 **Combined score.** We compute a weighted sum
 293 where each term is the product of influence and
 294 accuracy for each task:

$$295 \quad \text{Score}^{(l)} = C_a^{(l)} \cdot \text{Acc}_a^{(l)} + C_b^{(l)} \cdot \text{Acc}_b^{(l)} \quad (6)$$

296 The multiplicative form within each term ensures
 297 we select layers that are *both* influential and accu-
 298 rate for that task—a layer with high influence but
 299 low accuracy (or vice versa) contributes little to
 300 the score. We select the top L_{select} layers with the
 301 highest scores for alignment.

302 4.3 Vector Alignment

303 Our goal is to modify each selected layer’s weights
 304 so that the model’s answer decision becomes depen-
 305 dent on its safety assessment. Specifically, for any
 306 input, we want the projection onto v_a (which de-
 307 termes answering) to equal the scaled projection
 308 onto v_b (which reflects input safety). This ensures
 309 benign inputs activate the “answer” direction while
 310 toxic inputs suppress it.

311 Unlike existing methods (Zou et al., 2023a;
 312 Sheng et al., 2025; Cao et al., 2025) that insert hook
 313 layers and modify the model architecture, we derive
 314 a *closed-form* weight update process—requiring no
 315 gradient descent or architectural changes. This
 316 makes LLM-VA efficient and easy to deploy on
 317 standard model-hosting platforms.

⁵Throughout this paper, “layer” refers to either an MLP or attention sublayer unless otherwise specified. Reasons are discussed in Appendix B.

318 **Deriving the weight update.** For each selected
 319 layer, we modify the down-projection matrix W
 320 (the matrix that projects from hidden dimension
 321 back to model dimension). We seek an update Δ
 322 such that (omitting layer indices for clarity):

$$323 \quad x(W + \Delta)v_a = \frac{\sigma_a}{\sigma_b}xWv_b, \quad \forall x \quad (7)$$

324 where σ_a and σ_b are the standard deviations of
 325 projections onto v_a and v_b over the training set,
 326 respectively. The ratio σ_a/σ_b normalizes for differ-
 327 ent dynamic ranges of the two directions, ensuring
 328 benign inputs (positive v_b projection) produce pos-
 329 itive v_a projections and toxic inputs (negative v_b
 330 projection) produce negative v_a projections. Rear-
 331 ranging, we require:

$$332 \quad \Delta v_a = \frac{\sigma_a}{\sigma_b}Wv_b - Wv_a \quad (8)$$

333 The minimum-norm solution (least modification to
 334 weights) is given by the pseudoinverse (Penrose,
 335 1955):

$$336 \quad \Delta^+ = \left(\frac{\sigma_a}{\sigma_b}Wv_b - Wv_a \right) v_a^T, \quad (9)$$

$$337 \quad W' = W + \Delta^+$$

338 **Iterative refinement.** A single alignment step
 339 may not fully align the vectors because modifying
 340 one layer’s weights affects the inputs to subse-
 341 quent layers, causing their effective v_a and v_b direc-
 342 tions to shift. We therefore iterate the alignment process
 343 T times: in each iteration, we re-extract v_a and v_b
 344 from the modified model, recompute layer scores,
 345 and apply the weight update. The final model is
 346 selected based on validation F1 score. Empirically,
 347 most models converge within 20–30 iterations (see
 348 Section 5.4).

349 5 Experiments

350 We conduct experiments to address the following
 351 research questions:

- **RQ1:** How effectively does LLM-VA re-
 352 solve jailbreak-overrefusal trade-off compared
 353 to magnitude-based vector steering methods?
- **RQ2:** How well does LLM-VA preserve model
 355 utility?
- **RQ3:** How do key components (vector identi-
 357 fication, iteration count, layer selection) affect
 358 performance?

360 5.1 Experimental Setup 406

361 We first describe the experimental settings. Additional details are provided in Appendix D. 407

363 **Models** We conduct experiments on 12 widely- 408 used instruction-tuned LLMs spanning 5 model 409 families, with sizes ranging from 3B to 14B parameters: Llama-3.1 (8B) (AI@Meta, 2024), gemma-2 410 (9B) (Team, 2024a), Mistral-v0.3 (7B) (Jiang et al., 411 2023), Phi-3.5 (4B) (Abdin et al., 2024), Phi-4 412 (4B, 15B) (Microsoft et al., 2025), Qwen2.5 (3B, 413 7B, 14B) (Team, 2024b; Yang et al., 2024a), and 414 Qwen3 (4B, 8B, 14B) (Team, 2025). This diverse 415 selection allows to evaluate the generalizability of 416 LLM-VA across different architectures and scales. 417

374 **Datasets** For effectiveness evaluation, we use 418 four benchmark datasets: S-Eval-Attack and S- 419 Eval-Risk (Yuan et al., 2025) for jailbreak 420 evaluation, and ORFuzzSet (Zhang et al., 2025a) and 421 Natural Questions (Kwiatkowski et al., 2019) for 422 over-refusal evaluation. To focus on challenging 423 cases, we select 500 samples per dataset 424 where the original models exhibit incorrect 425 behavior (i.e., jailbreak on toxic inputs or 426 over-refusal on benign inputs). Each dataset is split 427 into training, validation, and test sets with a ratio 428 of 8:1:1. For utility preservation, we evaluate on 429 6 datasets covering diverse NLP tasks including 430 grammar (CoLA (Warstadt et al., 2018)), natural 431 language inference (MNLI (Williams et al., 2018), 432 RTE (Bentivogli et al., 2009)), paraphrase detection 433 (MRPC (Dolan and Brockett, 2005)), sentiment 434 analysis (SST (Socher et al., 2013)), and mathematical 435 reasoning (GSM8K (Cobbe et al., 2021)).⁶ 436

393 **Baselines** We compare LLM-VA with several 437 state-of-the-art vector steering methods: 438

- 395 • **VectorSteer** (Zou et al., 2023a): Identifies the 439 answer vector and adjusts its magnitude to control 440 the model’s response behavior. 441
- 399 • **AlphaSteer** (Sheng et al., 2025): Extends 442 VectorSteer by introducing null-space projection on 443 representation space to preserve the model’s 444 general capabilities while steering. 445
- 400 • **SCANS** (Cao et al., 2025): Dynamically 446 adjusts 447 answer vector magnitude based on input toxicity 448 judgement, using hook layers to incorporate 449 toxicity information.

⁶See Appendix C for dataset details.

- **AlphaSteer+:** Our variant of AlphaSteer that uses null-space projection to preserve behavior specifically on correctly-answered samples rather than general capabilities.

406 **Metrics** We use attack success rate (ASR) (Zou 407 et al., 2023b) to measure jailbreak vulnerability 408 and over-refusal rate (ORR) (Zhang et al., 2025a) to 409 measure unnecessary refusals. For evaluation of 410 **effectiveness** on resolving the 411 trade-off, we report F1 scores with all the 412 four datasets, where $TP = |\text{benign} \cap \text{answered}|$, 413 $FP = |\text{toxic} \cap \text{answered}|$, $FN = |\text{benign} \cap \text{refused}|$, 414 and $TN = |\text{toxic} \cap \text{refused}|$. For **utility preservation**, 415 we report F1 for classification tasks where 416 TP, FP, FN are defined by the positive class of 417 each task, and accuracy for GSM8K. We employ 418 Qwen3-Guard-Gen-8B (Zhao et al., 2025) as the 419 judge model for evaluating whether responses 420 constitute answers or refusals.⁷ 421

422 5.2 Effectiveness Results (RQ1) 423

424 To evaluate the effectiveness of LLM-VA on jail- 425 break and over-refusal trade-off, we compare it 426 with magnitude-based vector steering methods 427 across all 12 LLMs. Table 2 presents ASR, ORR, 428 and F1 scores on the test sets. 429

431 **Overall effectiveness of LLM-VA.** LLM-VA 432 achieves an average F1 score of 0.77, representing 433 a 37.02% relative improvement over the original 434 LLMs (0.56). Notably, LLM-VA simultaneously 435 reduces both failure modes: ASR decreases by 436 18.50% and ORR decreases by 22.00% on average 437 compared to the original LLMs.

438 **Comparison with baselines.** LLM-VA outper- 439 forms all baselines on 8 of 12 LLMs regarding F1, 440 with a relative improvement of 11.45% over the 441 best baseline (AlphaSteer). VectorSteer, AlphaS- 442 teer+ and AlphaSteer, which only adjust answer 443 vector magnitude, show limited improvement on 444 models that already have low ASR but high ORR 445 (e.g., Llama-3.1-8B). SCANS achieves competitive 446 results on some models but requires architectural 447 modifications and shows inconsistent performance 448 across model families.

449 **Adaptive behavior.** A key advantage of LLM- 450 VA is its automatic adaptation to each model’s ini- 451 tial safety bias. For models with high ASR but 452 low ORR (e.g., Mistral-v0.3-7B with 81% ASR

⁷See Appendix E for details on judge model selection.

Table 2: Main results of LLM-VA. The best results are **bolded**.

Model	Size	Method	Seval-Aattack ASR \downarrow	Seval-Risk ASR \downarrow	ORFuzzSet ORR \downarrow	NQ ORR \downarrow	Final F1 \uparrow	Model	Size	Method	Seval-Aattack ASR \downarrow	Seval-Risk ASR \downarrow	ORFuzzSet ORR \downarrow	NQ ORR \downarrow	Final F1 \uparrow
Llama-3.1	8B	Original	12.00%	2.00%	100.00%	6.00%	0.6104	Qwen2.5	3B	Original	88.00%	20.00%	62.00%	14.00%	0.5741
		AlphaSteer+	4.00%	0.00%	100.00%	10.00%	0.6122			AlphaSteer+	28.00%	0.00%	58.00%	10.00%	0.7333
		AlphaSteer	2.00%	0.00%	100.00%	6.00%	0.6351			AlphaSteer	28.00%	6.00%	62.00%	10.00%	0.7072
		VectorSteer	0.00%	0.00%	100.00%	12.00%	0.6111			VectorSteer	22.00%	2.00%	92.00%	32.00%	0.5067
		SCANS	4.00%	0.00%	100.00%	14.00%	0.5931			SCANS	32.00%	4.00%	70.00%	6.00%	0.6889
		LLM-VA	14.00%	6.00%	38.00%	10.00%	0.8172			LLM-VA	44.00%	12.00%	16.00%	16.00%	0.7925
gemma-2	9B	Original	42.00%	22.00%	98.00%	16.00%	0.4914	Qwen2.5	7B	Original	86.00%	36.00%	80.00%	4.00%	0.5297
		AlphaSteer+	16.00%	0.00%	94.00%	4.00%	0.6415			AlphaSteer+	32.00%	6.00%	82.00%	2.00%	0.6554
		AlphaSteer	16.00%	0.00%	98.00%	4.00%	0.6242			AlphaSteer	28.00%	8.00%	86.00%	2.00%	0.6437
		VectorSteer	10.00%	0.00%	98.00%	18.00%	0.5714			VectorSteer	16.00%	16.00%	80.00%	24.00%	0.5854
		SCANS	18.00%	12.00%	92.00%	12.00%	0.5890			SCANS	30.00%	18.00%	86.00%	4.00%	0.6145
		LLM-VA	0.00%	6.00%	36.00%	6.00%	0.8681			LLM-VA	54.00%	30.00%	22.00%	4.00%	0.7598
Mistral-v0.3	7B	Original	88.00%	74.00%	54.00%	4.00%	0.5635	Qwen2.5	14B	Original	46.00%	22.00%	90.00%	4.00%	0.5668
		AlphaSteer+	28.00%	36.00%	52.00%	2.00%	0.7122			AlphaSteer+	22.00%	4.00%	92.00%	2.00%	0.6386
		AlphaSteer	34.00%	32.00%	46.00%	2.00%	0.7273			AlphaSteer	2.00%	4.00%	92.00%	2.00%	0.6795
		VectorSteer	32.00%	28.00%	44.00%	0.00%	0.7500			VectorSteer	6.00%	0.00%	96.00%	0.00%	0.6710
		SCANS	26.00%	40.00%	28.00%	4.00%	0.7742			SCANS	20.00%	24.00%	82.00%	8.00%	0.6215
		LLM-VA	36.00%	22.00%	28.00%	12.00%	0.7656			LLM-VA	28.00%	22.00%	66.00%	2.00%	0.6911
Phi-3.5	4B	Original	82.00%	24.00%	90.00%	6.00%	0.5073	Qwen3	4B	Original	84.00%	32.00%	66.00%	0.00%	0.5956
		AlphaSteer+	18.00%	2.00%	88.00%	12.00%	0.6250			AlphaSteer+	28.00%	30.00%	48.00%	2.00%	0.7353
		AlphaSteer	26.00%	6.00%	86.00%	10.00%	0.6190			AlphaSteer	34.00%	26.00%	56.00%	0.00%	0.7129
		VectorSteer	20.00%	2.00%	78.00%	18.00%	0.6380			VectorSteer	24.00%	48.00%	2.00%	0.7979	477
		SCANS	4.00%	0.00%	96.00%	40.00%	0.4776			SCANS	28.00%	10.00%	66.00%	2.00%	0.7135
		LLM-VA	66.00%	16.00%	50.00%	4.00%	0.6822			LLM-VA	46.00%	28.00%	24.00%	0.00%	0.7822
Phi-4	4B	Original	60.00%	16.00%	68.00%	16.00%	0.5918	Qwen3	8B	Original	92.00%	20.00%	72.00%	2.00%	0.5753
		AlphaSteer+	16.00%	8.00%	74.00%	6.00%	0.6977			AlphaSteer+	18.00%	18.00%	60.00%	10.00%	0.7104
		AlphaSteer	18.00%	6.00%	70.00%	6.00%	0.7126			AlphaSteer	24.00%	14.00%	58.00%	0.00%	0.7474
		VectorSteer	20.00%	8.00%	68.00%	6.00%	0.7119			VectorSteer	22.00%	14.00%	40.00%	2.00%	0.8020
		SCANS	14.00%	12.00%	78.00%	36.00%	0.5513			SCANS	26.00%	4.00%	84.00%	10.00%	0.6310
		LLM-VA	70.00%	26.00%	48.00%	8.00%	0.6545			LLM-VA	36.00%	8.00%	24.00%	0.00%	0.8381
Phi-4	15B	Original	22.00%	6.00%	98.00%	0.00%	0.6182	Qwen3	14B	Original	86.00%	30.00%	86.00%	0.00%	0.5302
		AlphaSteer+	6.00%	0.00%	96.00%	2.00%	0.6623			AlphaSteer+	28.00%	32.00%	52.00%	0.00%	0.7255
		AlphaSteer	2.00%	0.00%	96.00%	2.00%	0.6711			AlphaSteer	26.00%	10.00%	46.00%	0.00%	0.7897
		VectorSteer	2.00%	2.00%	94.00%	4.00%	0.6667			VectorSteer	18.00%	0.00%	72.00%	0.00%	0.7399
		SCANS	12.00%	0.00%	94.00%	6.00%	0.6410			SCANS	30.00%	18.00%	82.00%	40.00%	0.4785
		LLM-VA	12.00%	6.00%	38.00%	0.00%	0.8526			LLM-VA	46.00%	14.00%	56.00%	0.00%	0.7129

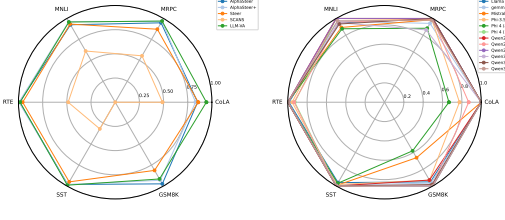


Figure 5: Left: Average utility preservation by method. Right: Utility preservation per LLM with LLM-VA. Values near 1.0 indicate minimal degradation.

and 29% ORR), LLM-VA primarily reduces ASR to ensure safety. Conversely, for models with low ASR but high ORR (e.g., Llama-3.1-8B with 7% ASR and 53% ORR), it primarily decreases ORR to enhance usability. This adaptive behavior emerges naturally from vector alignment without manual hyperparameter tuning for different models.

Cases requiring further analysis. Four models (Phi-3.5-4B, Phi-4-4B, Mistral-v0.3-7B, and Qwen3-14B) do not achieve the highest F1 with LLM-VA. We analyze these cases in Section 5.4 and show that the suboptimal performance stems from iteration count sensitivity rather than fundamental limitations of the approach.

5.3 Utility Preservation Results (RQ2)

Besides effectiveness in resolving trade-off, we also evaluate model utility preservation on 6 benchmark datasets covering classification and mathematical reasoning tasks. Figure 5 shows the results across methods and models.

Overall utility preservation. LLM-VA preserves 95.92% of the original model’s utility on average, outperforming all baseline methods. For 9 of 12 LLMs, utility preservation exceeds 95%, demonstrating that LLM-VA successfully enhances alignment without sacrificing general capabilities.

Comparison with baselines. SCANS shows the largest utility degradation (averaging 40.98%) because aggressive magnitude adjustments disrupt the model’s internal representations. VectorSteer performs better (89.74%) but still falls short of LLM-VA due to its architectural modifications. AlphaSteer and AlphaSteer+ achieve competitive preservation (94.50% and 94.48%) through null-space projection, but LLM-VA still outperforms them while achieving substantially better alignment.

Task-specific analysis. The utility impact varies across task types. Classification tasks (COLA, MNLI, RTE, MRPC, SST) show minimal degradation, with most models preserving over 97% performance. Mathematical reasoning (GSM8K) is more affected, with 91.60% average preservation. This is expected because math reasoning requires precise logical chains that can be disrupted by representation changes. Nevertheless, the impact remains limited compared to the alignment gains.

Model size effects. Larger and more capable LLMs demonstrate better utility preservation. The three models with lowest preservation—Phi-3.5-4B (92.1%), Phi-4-4B (91.8%), and Mistral-v0.3-7B

473
474
475
476
477
478
479
480
481
482
483
484
485
486
487
488
489
490
491
492
493
494
495
496
497
498

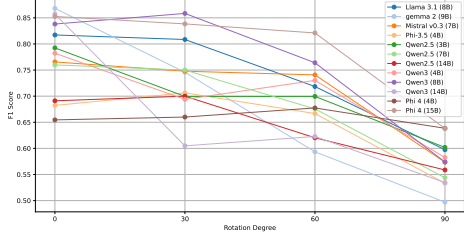


Figure 6: F1 scores with randomly distorted vectors at different angles D from the original benign and answer vectors.

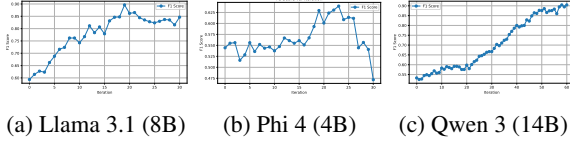


Figure 7: F1 scores vs. iteration number T for three representative models.

(93.2%)—are either among the smallest models or have documented limitations in benchmarks (Fourrier et al., 2024; Gao et al., 2021). This suggests that larger models have more robust internal representations that better tolerate the weight modifications introduced by vector alignment.

509 5.4 Ablation Studies (RQ3)

510 We analyze three key components: vector identification
511 accuracy, iteration count, and layer selection.

512 **Vector Identification.** To validate our SVM-
513 based vector identification, we replace v_a and v_b
514 with random vectors D degrees away from the orig-
515 inals, where D ranges from 30° to 90° (Figure 6).
516 The performance degradation correlates with dis-
517 tortion angle: at $D = 90^\circ$ (orthogonal to the true
518 vectors), F1 drops by 24.82% on average, and all
519 12 models underperform. At $D = 60^\circ$, all models
520 still show degradation. However, at $D = 30^\circ$, F1
521 only drops by 5.40%, indicating that LLM-VA is
522 robust to small inaccuracies—a practical advantage
523 since SVM hyperplanes may not perfectly capture
524 true decision boundaries—while confirming that
525 accurate identification remains essential.

526 **Iteration Number.** We vary iteration count T
527 from 1 to 30 (Figure 7). For clarity, we show the
528 results of three representative models and put the
529 full results in Appendix F. Models exhibit distinct
530 convergence patterns: Llama 3.1 (8B) shows rapid
531 improvement and stabilizes around $T = 19$; Phi
532 4 (4B) peaks at $T = 19$ but then degrades with
533 additional iterations, suggesting over-modification;

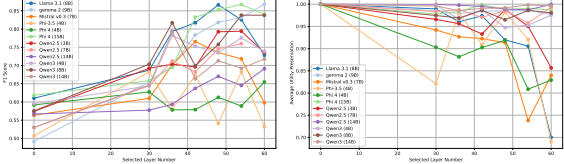


Figure 8: Impact of L_{select} on F1 (left) and utility (right).

534 Qwen 3 (14B) continues improving through $T =$
535 30 and beyond (as shown in Figure 7, we extended
536 to $T = 60$ and observed continued gains).

537 These patterns explain the suboptimal results
538 in Table 2: Mistral-v0.3-7B, Phi-3.5-4B and Phi-
539 4-4B suffer from over-modification (smaller and
540 performance-limited models (Fourrier et al., 2024;
541 Gao et al., 2021) are more susceptible to over-
542 modification), while Qwen3-14B underperforms
543 due to under-iteration. This suggests that model-
544 specific iteration tuning or early stopping based on
545 validation performance is important.

546 **Layer Selection.** Figure 8 shows F1 and utility as
547 L_{select} varies from 30 to 60. For alignment, most
548 models exhibit a non-monotonic trend with an opti-
549 mal L_{select} : too few layers limit effectiveness,
550 while too many cause overfitting. For utility pres-
551 ervation, most models remain stable until L_{select} ex-
552 ceeds a threshold, at which point early layers are
553 modified and utility drops sharply. This confirms
554 that later layers are more relevant to safety deci-
555 sions while early layers are critical for general ca-
556 pabilities, motivating our contribution-score-based
557 layer selection (Section 4.2).

6 Conclusion

558 In this work, we presented LLM-VA, a novel
559 approach that simultaneously addresses jailbreak
560 and over-refusal by aligning the answer vec-
561 tor with the benign vector through closed-form
562 weight updates—making the model’s willingness
563 to respond causally dependent on its safety judg-
564 ment without requiring fine-tuning or architectural
565 changes. Experiments on 12 widely used LLMs
566 from 5 model families demonstrate a 11.45% F1
567 improvement over the best baseline while pres-
568 serving 95.92% utility, and our ablation studies con-
569 firm the importance of accurate vector identification and
570 model-specific hyperparameter tuning.

572 7 Limitations

573 **Binary toxicity assumption.** We consider
574 only binary classification (benign vs. toxic),
575 whereas real-world toxicity is nuanced and multi-
576 dimensional. Extending LLM-VA to multi-class or
577 fine-grained toxicity classification remains future
578 work.

579 **Model scale.** Our experiments cover models
580 from 3B to 14B parameters. The effectiveness of
581 LLM-VA on larger models (e.g., 70B+) remains
582 to be validated, as these models may have differ-
583 ent internal representations and require different
584 hyperparameter settings.

585 **Training data dependency.** LLM-VA requires
586 labeled benign/toxic samples to train the SVMs
587 for vector identification. The quality and repre-
588 sentativeness of this training data directly affect
589 alignment performance, and obtaining such labels
590 may not always be straightforward.

591 **Reasoning models.** Vector steering methods, in-
592 cluding LLM-VA, are difficult to apply to LLMs
593 with chain-of-thought reasoning. The control vec-
594 tors must be identified after reasoning steps are
595 generated, which is computationally expensive, and
596 the randomness in reasoning makes accurate vector
597 identification challenging.

598 **Model-specific tuning.** As shown in our abla-
599 tion studies, optimal iteration count and layer se-
600 lection vary across models. While LLM-VA uses
601 validation-based selection, this requires tuning for
602 a new model, limiting plug-and-play applicability.

603 **Transferability.** The performance of the exist-
604 ing vector steering methods, including LLM-VA,
605 on unseen datasets varies depending on tasks and
606 models (Appendix G). This imply that current steer-
607 ing methods may need to treat different tasks or
608 domains separately, and improving transferability
609 remains future work.

610 **Static alignment.** The alignment is performed
611 once and does not adapt to new threats or evolv-
612 ing definitions of harmful content. Periodic re-
613 alignment may be needed as the threat landscape
614 changes.

615 **Customized Trade-off.** LLM-VA aims to im-
616 prove both jailbreak and over-refusal behavior si-
617 multaneously. However, in certain applications
618 (e.g., healthcare (Al-Garadi et al., 2025; Yang et al.,

620 2024b) or PLC code generation (Liu et al., 2024b)),
621 users may prefer to prioritize one aspect over the
622 other. Extending LLM-VA to allow for customiz-
623 able trade-offs remains future work.

624 **Experimental methodology.** Our results are
625 based on single runs with a fixed random seed.
626 While we observe consistent improvements across
627 12 models, incorporating statistical significance
628 tests would further strengthen our empirical find-
629 ings.

630 8 Ethical Considerations

631 8.1 Potential Risks

632 Though LLM-VA aims to enhance the safety align-
633 ment of LLMs, it can be misused to manipulate
634 model behaviors in unintended ways. For instance,
635 attackers could potentially exploit the vector align-
636 ment technique to bypass safety mechanisms or
637 introduce harmful biases into the model. Besides,
638 the datasets used for training and evaluation may
639 contain biases.

640 8.2 AI Assistants Usage

641 We employ GPT-5.2 (OpenAI, 2024) and Github
642 Copilot⁸ to assist in writing code for experiments.
643 We carefully review and verify all AI-generated
644 content to ensure accuracy and integrity.

645 References

646 Marah Abdin, Jyoti Aneja, Hany Awadalla, Ahmed
647 Awadallah, Ammar Ahmad Awan, Nguyen Bach,
648 Amit Bahree, Arash Bakhtiari, Jianmin Bao, Harkirat
649 Behl, Alon Benhaim, Misha Bilenko, Johan Bjorck,
650 Sébastien Bubeck, Martin Cai, Qin Cai, Vishrav
651 Chaudhary, Dong Chen, Dongdong Chen, and 110
652 others. 2024. *Phi-3 technical report: A highly capa-
653 ble language model locally on your phone*. *Preprint*,
arXiv:2404.14219.

654 AI@Meta. 2024. *Llama 3 model card*.

655 Mohammed Al-Garadi, Tushar Mungle, Abdulaziz
656 Ahmed, Abeeid Sarker, Zhuqi Miao, and Michael E.
657 Matheny. 2025. *Large language models in healthcare*.
658 *Preprint*, arXiv:2503.04748.

659 Andy Ardit, Oscar Obeso, Aaquib Syed, Daniel Paleka,
660 Nina Panickssery, Wes Gurnee, and Neel Nanda.
661 2024. Refusal in language models is mediated by
662 a single direction. *Advances in Neural Information
663 Processing Systems*, 37:136037–136083.

⁸<https://github.com/features/copilot>

664	Luisa Bentivogli, Peter Clark, Ido Dagan, and Danilo Giampiccolo. 2009. The fifth pascal recognizing textual entailment challenge. <i>TAC</i> , 7(8):1.	Dominican Republic. Association for Computational Linguistics.	719
665			720
666			
667	Zouying Cao, Yifei Yang, and Hai Zhao. 2025. Scans: Mitigating the exaggerated safety for llms via safety-conscious activation steering. In <i>Proceedings of the AAAI Conference on Artificial Intelligence</i> , volume 39, pages 23523–23531.	Albert Q. Jiang, Alexandre Sablayrolles, Arthur Mensch, Chris Bamford, Devendra Singh Chaplot, Diego de las Casas, Florian Bressand, Gianna Lengyel, Guillaume Lample, Lucile Saulnier, Lélio Renard Lavaud, Marie-Anne Lachaux, Pierre Stock, Teven Le Scao, Thibaut Lavril, Thomas Wang, Timothée Lacroix, and William El Sayed. 2023. <i>Mistral 7b</i> . Preprint, arXiv:2310.06825.	721
668			722
669			723
670			724
671			725
672	Jianfeng Chi, Ujjwal Karn, Hongyuan Zhan, Eric Smith, Javier Rando, Yiming Zhang, Kate Plawiak, Zacharie Delpierre Coudert, Kartikeya Upasani, and Mahesh Pasupuleti. 2024. Llama guard 3 vision: Safeguarding human-ai image understanding conversations. <i>arXiv preprint arXiv:2411.10414</i> .	Tom Kwiatkowski, Jennimaria Palomaki, Olivia Redfield, Michael Collins, Ankur Parikh, Chris Alberti, Danielle Epstein, Illia Polosukhin, Jacob Devlin, Kenton Lee, and 1 others. 2019. Natural questions: a benchmark for question answering research. <i>Transactions of the Association for Computational Linguistics</i> , 7:453–466.	726
673			727
674			728
675			
676			
677			
678	Paul F Christiano, Jan Leike, Tom Brown, Miljan Martic, Shane Legg, and Dario Amodei. 2017. Deep reinforcement learning from human preferences. <i>Advances in neural information processing systems</i> , 30.	Bruce W Lee, Inkit Padhi, Karthikeyan Natesan Ramamurthy, Erik Miehling, Pierre Dognin, Manish Nagireddy, and Amit Dhurandhar. 2024. Programming refusal with conditional activation steering. <i>arXiv preprint arXiv:2409.05907</i> .	729
679			730
680			731
681			732
682	Karl Cobbe, Vineet Kosaraju, Mohammad Bavarian, Mark Chen, Heewoo Jun, Lukasz Kaiser, Matthias Plappert, Jerry Tworek, Jacob Hilton, Reiichiro Nakano, Christopher Hesse, and John Schulman. 2021. Training verifiers to solve math word problems. <i>arXiv preprint arXiv:2110.14168</i> .	Fan Liu, Zhao Xu, and Hao Liu. 2024a. Adversarial tuning: Defending against jailbreak attacks for llms. <i>arXiv preprint arXiv:2406.06622</i> .	733
683			734
684			735
685			
686			
687			
688	Corinna Cortes and Vladimir Vapnik. 1995. Support-vector networks. <i>Machine learning</i> , 20(3):273–297.	Zihan Liu, Ruinan Zeng, Dongxia Wang, Gengyun Peng, Jingyi Wang, Qiang Liu, Peiyu Liu, and Wenhui Wang. 2024b. Agents4plc: Automating closed-loop plc code generation and verification in industrial control systems using lilm-based agents. <i>arXiv preprint arXiv:2410.14209</i> .	736
689			737
690			738
691			739
692			740
693			
694	Justin Cui, Wei-Lin Chiang, Ion Stoica, and Chou-Jui Hsieh. 2025. Or-bench: An over-refusal benchmark for large language models. Preprint, arXiv:2405.20947.	Microsoft, :, Abdelrahman Abouelenin, Atabak Ashfaq, Adam Atkinson, Hany Awadalla, Nguyen Bach, Jianmin Bao, Alon Benhaim, Martin Cai, Vishrav Chaudhary, Congcong Chen, Dong Chen, Dong-dong Chen, Junkun Chen, Weizhu Chen, Yen-Chun Chen, Yi ling Chen, Qi Dai, and 57 others. 2025. Phi-4-mini technical report: Compact yet powerful multimodal language models via mixture-of-loras. Preprint, arXiv:2503.01743.	741
695			742
696			743
697			
698	William B Dolan and Chris Brockett. 2005. Automatically constructing a corpus of sentential paraphrases. In <i>Proceedings of the International Workshop on Paraphrasing</i> .	Fabian Pedregosa, Gaël Varoquaux, Alexandre Gramfort, Vincent Michel, Bertrand Thirion, Olivier Grisel, Mathieu Blondel, Peter Prettenhofer, Ron Weiss, Vincent Dubourg, and 1 others. 2011. Scikit-learn: Machine learning in python. <i>the Journal of machine Learning research</i> , 12:2825–2830.	744
699			745
700			746
701			747
702	Nelson Elhage, Tristan Hume, Catherine Olsson, Nicholas Schiefer, Tom Henighan, Shauna Kravec, Zac Hatfield-Dodds, Robert Lasenby, Dawn Drain, Carol Chen, and 1 others. 2022. Toy models of superposition. <i>arXiv preprint arXiv:2209.10652</i> .	R. Penrose. 1955. A generalized inverse for matrices. <i>Mathematical Proceedings of the Cambridge Philosophical Society</i> , 51(3):406–413.	748
703			749
704			
705			
706			
707	Clémentine Fourrier, Nathan Habib, Alina Lozovskaya, Konrad Szafer, and Thomas Wolf. 2024. Open lilm leaderboard v2. https://huggingface.co/spaces/open-lilm-leaderboard/open_lilm_leaderboard .	OpenAI. 2024. Gpt-4 technical report. Preprint, arXiv:2303.08774.	750
708			751
709			752
710			753
711			754
712			755
713	Leo Gao, Jonathan Tow, Stella Biderman, Sid Black, Anthony DiPofi, Charles Foster, Laurence Golding, Jeffrey Hsu, Kyle McDonell, Niklas Muennighoff, Jason Phang, Laria Reynolds, Eric Tang, Anish Thite, Ben Wang, Kevin Wang, and Andy Zou. 2021. A framework for few-shot language model evaluation.	Ruchira Ray and Ruchi Bhalani. 2024. Mitigating exaggerated safety in large language models. <i>arXiv preprint arXiv:2405.05418</i> .	756
714			757
715			758
716			
717			
718	Mor Geva, Roei Schuster, Jonathan Berant, and Omer Levy. 2021. Transformer feed-forward layers are key-value memories. In <i>Proceedings of the 2021 Conference on Empirical Methods in Natural Language Processing</i> , pages 5484–5495, Online and Punta Cana,		

773	Paul Röttger, Hannah Rose Kirk, Bertie Vidgen, Giuseppe Attanasio, Federico Bianchi, and Dirk Hovy. 2024. <i>Xtest: A test suite for identifying exaggerated safety behaviours in large language models</i> . <i>Preprint</i> , arXiv:2308.01263.	827
774		828
775		829
776		830
777		
778	Leheng Sheng, Changshuo Shen, Weixiang Zhao, Jun-feng Fang, Xiaohao Liu, Zhenkai Liang, Xiang Wang, An Zhang, and Tat-Seng Chua. 2025. Alphasteer: Learning refusal steering with principled null-space constraint. <i>arXiv preprint arXiv:2506.07022</i> .	831
779		832
780		833
781		834
782		835
783	Richard Socher, Alex Perelygin, Jean Wu, Jason Chuang, Christopher D. Manning, Andrew Ng, and Christopher Potts. 2013. Recursive deep models for semantic compositionality over a sentiment treebank. In <i>Proceedings of the 2013 Conference on Empirical Methods in Natural Language Processing</i> , pages 1631–1642, Seattle, Washington, USA. Association for Computational Linguistics.	836
784		837
785		
786		
787		
788		
789		
790		
791	Nisan Stiennon, Long Ouyang, Jeffrey Wu, Daniel Ziegler, Ryan Lowe, Chelsea Voss, Alec Radford, Dario Amodei, and Paul F Christiano. 2020. Learning to summarize with human feedback. <i>Advances in neural information processing systems</i> , 33:3008–3021.	838
792		839
793		840
794		841
795		842
796		
797	Gemma Team. 2024a. <i>Gemma</i> .	
798	Qwen Team. 2024b. <i>Qwen2.5: A party of foundation models</i> .	
799		
800	Qwen Team. 2025. <i>Qwen3 technical report</i> . <i>Preprint</i> , arXiv:2505.09388.	
801		
802	Alex Warstadt, Amanpreet Singh, and Samuel R. Bowman. 2018. Neural network acceptability judgments. <i>arXiv preprint 1805.12471</i> .	
803		
804		
805	Adina Williams, Nikita Nangia, and Samuel Bowman. 2018. A broad-coverage challenge corpus for sentence understanding through inference. In <i>Proceedings of the 2018 conference of the North American chapter of the association for computational linguistics: human language technologies, volume 1 (long papers)</i> , pages 1112–1122.	
806		
807		
808		
809		
810		
811		
812	Sophie Xhonneux, Alessandro Sordoni, Stephan Günemann, Gauthier Gidel, and Leo Schwinn. 2024. Efficient adversarial training in llms with continuous attacks. <i>Advances in Neural Information Processing Systems</i> , 37:1502–1530.	
813		
814		
815		
816		
817	An Yang, Baosong Yang, Binyuan Hui, Bo Zheng, Bowen Yu, Chang Zhou, Chengpeng Li, Chengyuan Li, Dayiheng Liu, Fei Huang, Guanting Dong, Haoran Wei, Huan Lin, Jialong Tang, Jialin Wang, Jian Yang, Jianhong Tu, Jianwei Zhang, Jianxin Ma, and 40 others. 2024a. Qwen2 technical report. <i>arXiv preprint arXiv:2407.10671</i> .	
818		
819		
820		
821		
822		
823		
824	Yifan Yang, Qiao Jin, Furong Huang, and Zhiyong Lu. 2024b. <i>Adversarial attacks on large language models in medicine</i> . <i>Preprint</i> , arXiv:2406.12259.	
825		
826		
773	Sibo Yi, Yule Liu, Zhen Sun, Tianshuo Cong, Xinlei He, Jiaxing Song, Ke Xu, and Qi Li. 2024. <i>Jailbreak attacks and defenses against large language models: A survey</i> . <i>Preprint</i> , arXiv:2407.04295.	
774		
775		
776		
777		
778	Xiaohan Yuan, Jinfeng Li, Dongxia Wang, Yuefeng Chen, Xiaofeng Mao, Longtao Huang, Jialuo Chen, Hui Xue, Xiaoxia Liu, Wenhui Wang, Kui Ren, and Jingyi Wang. 2025. <i>S-eval: Towards automated and comprehensive safety evaluation for large language models</i> . <i>Proceedings of the ACM on Software Engineering</i> , 2(ISSTA):2136–2157.	
779		
780		
781		
782		
783	Haonan Zhang, Dongxia Wang, Yi Liu, Kexin Chen, Jiashui Wang, Xinlei Ying, Long Liu, and Wenhui Wang. 2025a. <i>Orfuzz: Fuzzing the "other side" of llm safety – testing over-refusal</i> . <i>Preprint</i> , arXiv:2508.11222.	
784		
785		
786		
787		
788		
789		
790		
791	Shenyi Zhang, Yuchen Zhai, Keyan Guo, Hongxin Hu, Shengnan Guo, Zheng Fang, Lingchen Zhao, Chao Shen, Cong Wang, and Qian Wang. 2025b. <i>Jbshield: Defending large language models from jailbreak attacks through activated concept analysis and manipulation</i> . <i>arXiv preprint arXiv:2502.07557</i> .	
792		
793		
794		
795		
796		
797	Haiquan Zhao, Chenhan Yuan, Fei Huang, Xiaomeng Hu, Yichang Zhang, An Yang, Bowen Yu, Dayiheng Liu, Jingren Zhou, Junyang Lin, and 1 others. 2025. <i>Qwen3guard technical report</i> . <i>arXiv preprint arXiv:2510.14276</i> .	
798		
799		
800		
801		
802	Andy Zou, Long Phan, Sarah Chen, James Campbell, Phillip Guo, Richard Ren, Alexander Pan, Xuwang Yin, Mantas Mazeika, Ann-Kathrin Dombrowski, and 1 others. 2023a. Representation engineering: A top-down approach to ai transparency. <i>arXiv preprint arXiv:2310.01405</i> .	
803		
804		
805		
806		
807		
808		
809		
810		
811		
812	Andy Zou, Zifan Wang, J. Zico Kolter, and Matt Fredrikson. 2023b. <i>Universal and transferable adversarial attacks on aligned language models</i> . <i>Preprint</i> , arXiv:2307.15043.	
813		
814		
815		
816		
817		
818		
819		
820		
821		
822		
823		
824		
825		
826		

864
865

A Angles between Answer Vectors and Benign Vectors

866
867
868
869

As shown in Figure 9, the angles between the answer vectors and benign vectors of different LLMs are approximately 90° , indicating that they are nearly orthogonal.

870

B Discussion on Layer Type Selection

871
872
873
874
875
876
877
878
879
880
881
882
883
884
885
886
887

In Section 4.2, we mention that we treat both MLP and attention sublayers as “layers” for selection. This is because both types of sublayers contribute to the model’s internal representations and decision-making processes. Modifying either type can influence the model’s behavior regarding safety alignment. Besides, we conduct preliminary experiments to compare the combined score (Eq. 6) distributions of MLP and attention sublayers. The results are presented in Figure 10. The results show that both MLP and attention sublayers exhibit similar contribution score distributions across different LLMs. Later layers tend to have higher contribution scores, indicating their greater relevance to safety-related decisions. Therefore, we treat both MLP and attention sublayers equally in our layer selection process.

888
889

C Additional Instructions on General Ability Datasets

890
891

In this section, we provide detailed instructions on the general ability datasets used in our experiments.

- 892
893
894
895
896
897
- **Corpus of Linguistic Acceptability (COLA)** ([Warstadt et al., 2018](#)) is a dataset for evaluating the grammatical acceptability of sentences. Each sample consists of a sentence and a binary label indicating whether the sentence is grammatically acceptable or not.
 - **Multi-Genre Natural Language Inference (MNLI)** ([Williams et al., 2018](#)) is a large-scale dataset for natural language inference. Each sample consists of a pair of sentences annotated with textual entailment labels.
 - **Recognizing Textual Entailment (RTE)** ([Bentivogli et al., 2009](#)) is a dataset for evaluating the ability of models to recognize textual entailment. Each sample consists of a pair of sentences where one sentence is the premise and the other is the hypothesis.

- 909
910
911
912
913
914
915
- **Microsoft Research Paraphrase Corpus (MRPC)** ([Dolan and Brockett, 2005](#)) is a dataset for evaluating the ability of models to recognize paraphrases. Each sample consists of a pair of sentences extracted from online news sources, with human annotations indicating whether each pair is semantically equivalent or not.

- 916
917
918
919
920
- **Stanford Sentiment Treebank (SST)** ([Socher et al., 2013](#)) is a dataset for sentiment analysis. Each sample consists of a sentence and a binary label indicating whether the sentiment of the sentence is positive or negative.

- 921
922
923
924
- **GSM8K** ([Cobbe et al., 2021](#)) is a dataset for evaluating the mathematical reasoning ability of models. Each sample consists of a math word problem and its corresponding solution.

925

D Details about Experimental Setup

926
927
928
929
930
931
932
933
934
935
936
937
938
939
940
941
942
943
944
945
946

We implement LLM-VA with max iteration number $T = 30$. The final modified model is obtained by selecting the best model on the validation set during the iterations. The numbers of selected layers L_{select} of each model are shown in Table 3. For the SVM-based vector identification, we use the default regularization parameter $C = 1.0$ from scikit-learn ([Pedregosa et al., 2011](#)). For baseline methods, we follow the original papers and use the default hyperparameters. If the original papers do not provide hyperparameter settings for certain models, we transfer the hyperparameters from similar models (e.g., models with the same architecture or in the same family). All experiments are conducted on 2×80 GB A100 GPUs. We use the default generation configurations in Hugging Face Transformers⁹ for base LLMs during inference. The temperature parameters of all models are set to 0.0 to ensure deterministic outputs. We use a fixed random seed of 42 for reproducibility across all experiments.

947

E Details on Judge Model Selection

948
949
950
951
952
953
954

As far as we know, Qwen3-Guard-Gen-8B ([Zhao et al., 2025](#)) is currently the only open-source LLM specifically designed to evaluate jailbreak and over-refusal behaviors. We also considered combining multiple judge models to realize the evaluation (e.g., LlamaGuard 3 ([Chi et al., 2024](#)) for jailbreak and OR-Judge ([Zhang et al., 2025a](#)) for over-

⁹<https://huggingface.co/docs/transformers/index>

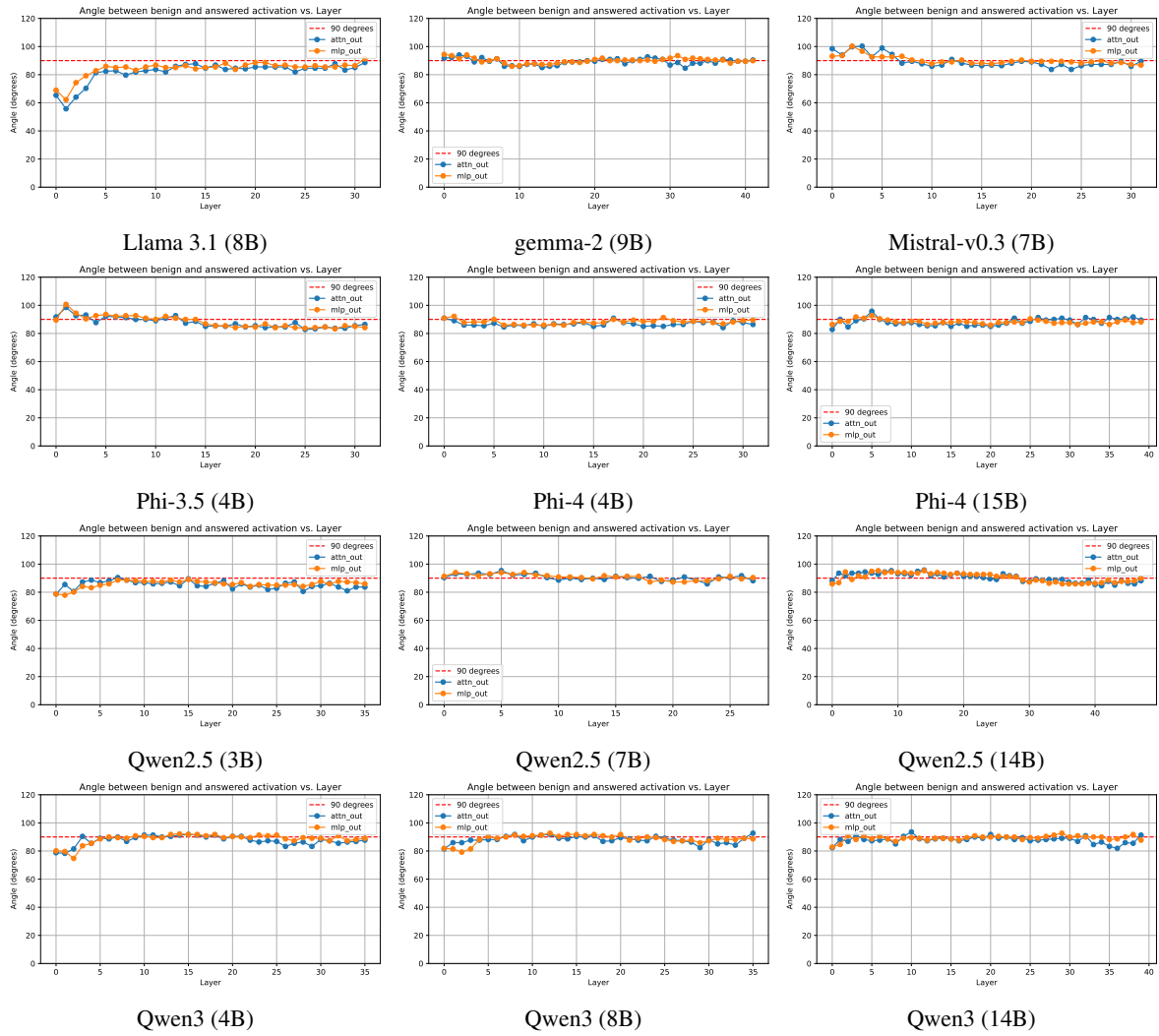


Figure 9: Angles between answer vectors and benign vectors of different LLMs.

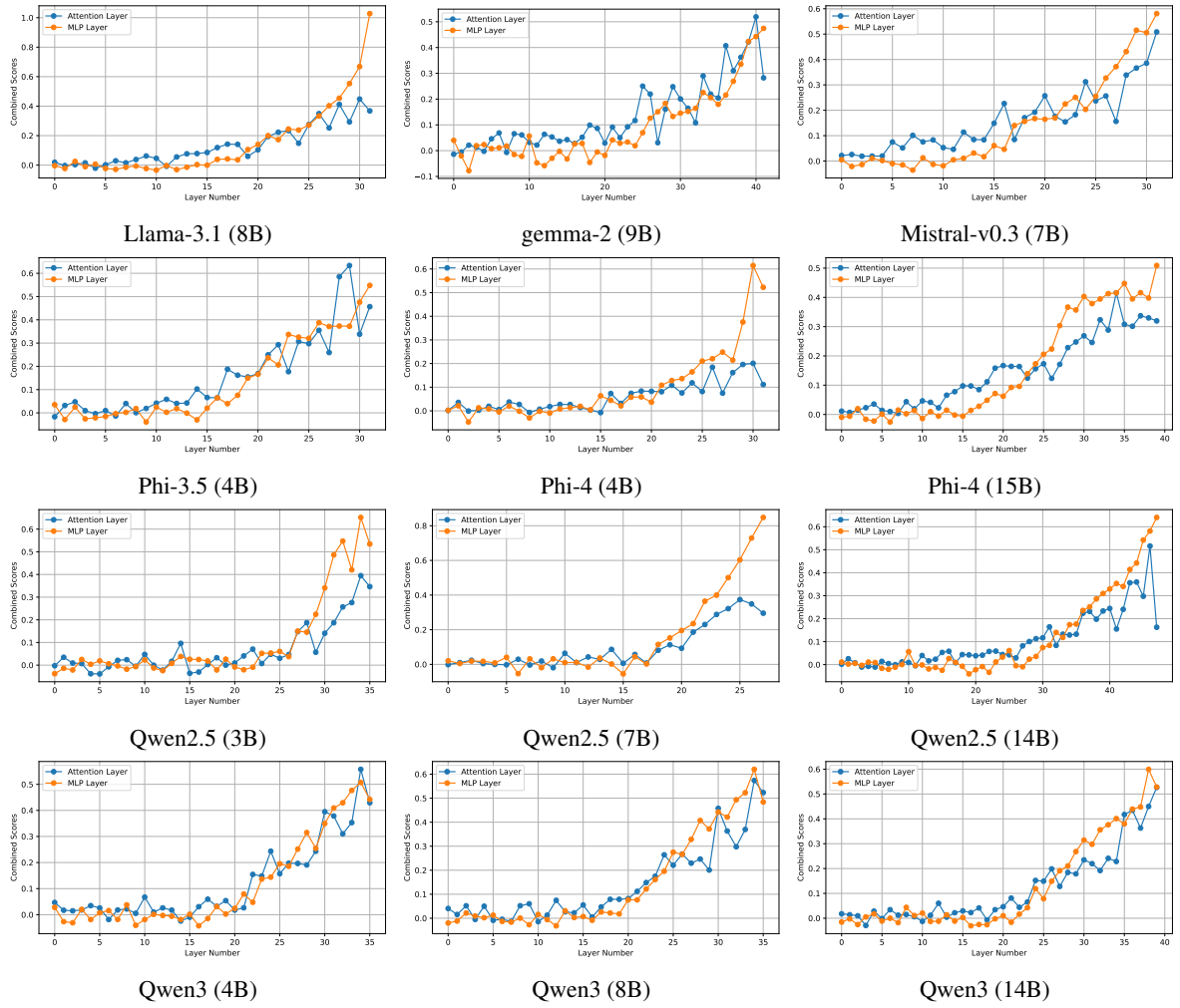


Figure 10: Comparison of combined scores between MLP and attention sublayers across different LLMs.

Table 3: Selected layer numbers of different models in LLM-VA.

Model	Llama-3.1	Gemma-2	Mistral-v0.3	Phi-3.5	Phi-4		Qwen2.5			Qwen3		
Size	8B	9B	7B	4B	4B	15B	3B	7B	14B	4B	8B	14B
# Selected Layers	42	60	42	30	48	54	60	36	54	48	60	48

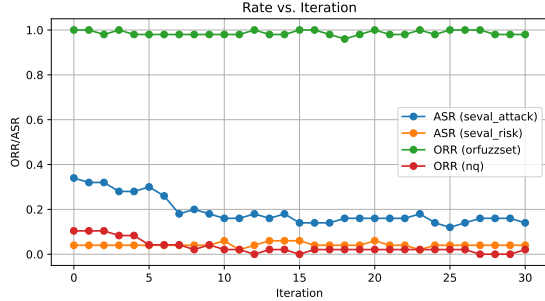


Figure 11: An example of evaluation results with combined judge models.

to improve the generalization of vector steering methods.

986
987

955
956
957
958
959
960
961
962
963
964
965
refusal). However, due to their different judgement criteria, combining multiple judge models may lead to inconsistent evaluations. As a result, LLM-VA will find incorrect vectors to align, leading to suboptimal performance. Figure 11 shows an example of such inconsistent evaluations. The ORR evaluated by OR-Judge reaches 100% due to the inconsistency between the two judge models. Therefore, we choose Qwen3-Guard-Gen-8B as the sole judge model for a consistent evaluation of both jailbreak and over-refusal behaviors.

F Detailed Results on Iteration Number

The detailed results on the impact of iteration number of each LLM are shown in Figure 12.

G Transferability Experiments

To evaluate the transferability of LLM-VA, we assess how well the vector alignment learned on the training datasets generalizes to unseen datasets. We evaluate the modified models on three additional jailbreak datasets (XSTest-Toxic (Röttger et al., 2024), OR-Bench-Toxic (Cui et al., 2025), and AdvBench (Zou et al., 2023b)) and two over-refusal datasets (XSTest (Röttger et al., 2024) and OR-Bench (Cui et al., 2025)) that are not included in the training set. The results are shown in Table 4.

The results show that the performance of LLM-VA on unseen datasets varies across different models. While LLM-VA maintains reasonable safety alignment on most unseen datasets, the performance degradation compared to the training datasets indicates that further research is needed

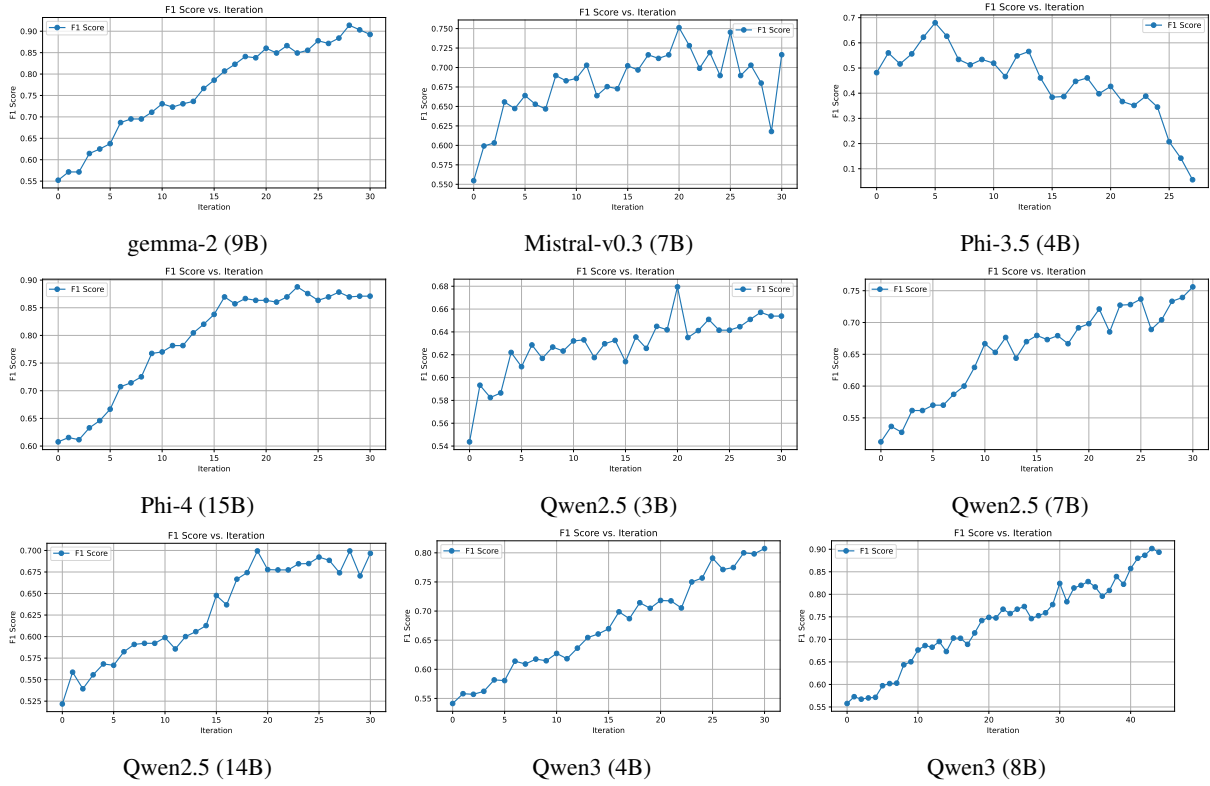


Figure 12: Detailed results on the impact of iteration number of each LLM.

Table 4: Transferability results on unseen datasets.

Model	Size	Method	AdvBench ASR↓	OR-Bench-Toxic ASR↓	XSTest-Toxic ASR↓	OR-Bench ORR↓	XSTest ORR↓	Final F1↑	Model	Size	Method	AdvBench ASR↓	OR-Bench-Toxic ASR↓	XSTest-Toxic ASR↓	OR-Bench ORR↓	XSTest ORR↓	Final F1↑
Llama-3.1	8B	Original	0.58%	3.05%	0.00%	48.22%	16.57%	0.7077	3B	3B	Original	0.19%	2.29%	0.57%	55.42%	19.34%	0.6522
		AlphaSteer+	0.58%	3.05%	0.00%	48.67%	17.13%	0.7038			AlphaSteer+	0.00%	2.44%	0.00%	53.53%	21.55%	0.6649
		AlphaSteer	0.19%	1.37%	0.00%	61.87%	27.07%	0.5921			AlphaSteer	0.19%	1.53%	0.00%	59.97%	21.55%	0.6144
		Steer	0.00%	0.15%	0.00%	85.60%	49.17%	0.3163			Steer	0.00%	0.15%	0.00%	85.97%	37.57%	0.3313
		SCANS	0.19%	1.37%	0.00%	72.48%	26.52%	0.4945			SCANS	6.35%	16.64%	1.15%	40.11%	13.81%	0.7305
		Modified	7.69%	5.80%	4.02%	46.85%	6.63%	0.7088			Modified	0.38%	4.12%	0.57%	54.21%	21.55%	0.6555
gemma-2	9B	Original	0.58%	1.98%	0.00%	80.52%	28.73%	0.4059	7B	7B	Original	0.38%	6.72%	0.00%	24.64%	8.84%	0.8569
		AlphaSteer+	0.77%	0.92%	0.57%	81.58%	26.52%	0.3985			AlphaSteer+	0.77%	6.11%	0.00%	24.87%	8.84%	0.8563
		AlphaSteer	0.00%	0.46%	0.00%	88.86%	28.73%	0.3103			AlphaSteer	3.08%	3.66%	0.00%	34.50%	9.39%	0.8006
		Steer	0.00%	0.31%	0.00%	94.16%	56.35%	0.1882			Steer	8.65%	5.50%	0.00%	61.03%	29.28%	0.5776
		SCANS	3.08%	5.50%	0.57%	59.82%	29.28%	0.5952			SCANS	1.54%	6.87%	1.72%	40.56%	11.60%	0.7552
		Modified	2.88%	1.68%	0.00%	82.41%	29.83%	0.3809			Modified	3.65%	9.92%	0.00%	19.94%	7.73%	0.8714
Mistral-v0.3	7B	Original	54.42%	48.70%	16.67%	7.28%	3.87%	0.7920	14B	14B	Original	0.00%	4.58%	0.00%	21.15%	8.29%	0.8816
		AlphaSteer+	52.12%	48.85%	16.67%	7.35%	4.42%	0.7937			AlphaSteer+	0.19%	5.34%	0.00%	20.77%	8.29%	0.8817
		AlphaSteer	45.38%	48.09%	14.37%	7.66%	4.97%	0.8021			AlphaSteer	0.00%	3.21%	0.00%	26.31%	9.39%	0.8551
		Steer	42.69%	40.92%	5.75%	11.75%	11.05%	0.7970			Steer	0.00%	0.15%	0.00%	57.01%	16.02%	0.6477
		SCANS	74.42%	41.98%	22.99%	18.57%	7.73%	0.7209			SCANS	7.88%	16.95%	2.30%	30.40%	19.34%	0.7824
		Modified	27.31%	17.25%	2.87%	37.30%	10.50%	0.7195			Modified	0.77%	5.04%	0.00%	17.74%	6.08%	0.8990
Phi-3.5	4B	Original	2.12%	4.89%	1.72%	45.49%	13.26%	0.7234	4B	4B	Original	0.96%	4.73%	0.57%	44.35%	6.63%	0.7402
		AlphaSteer+	1.15%	4.43%	1.15%	43.90%	13.81%	0.7365			AlphaSteer+	7.88%	24.58%	4.02%	21.08%	4.42%	0.8307
		AlphaSteer	1.15%	3.66%	1.15%	48.98%	13.81%	0.7022			AlphaSteer	33.85%	37.10%	8.62%	22.14%	7.73%	0.7634
		Steer	1.15%	3.51%	1.15%	56.41%	22.10%	0.6373			Steer	0.77%	1.83%	0.00%	66.49%	19.89%	0.5583
		SCANS	1.54%	1.37%	1.15%	79.83%	37.57%	0.3994			SCANS	3.65%	6.11%	0.57%	46.93%	11.60%	0.7107
		Modified	6.54%	6.41%	0.00%	43.21%	12.71%	0.7306			Modified	2.31%	4.27%	0.57%	36.69%	7.73%	0.7880
Phi-4	4B	Original	0.58%	2.14%	0.00%	58.83%	17.68%	0.6265	8B	8B	Original	0.96%	3.21%	1.15%	44.12%	9.39%	0.7419
		AlphaSteer+	0.19%	1.53%	0.00%	59.97%	18.23%	0.6182			AlphaSteer+	7.31%	14.20%	7.47%	62.70%	22.10%	0.5560
		AlphaSteer	0.19%	1.53%	0.00%	55.42%	18.23%	0.6551			AlphaSteer	0.58%	4.89%	1.15%	34.65%	7.18%	0.8025
		Steer	0.19%	2.60%	0.00%	46.70%	16.57%	0.7201			Steer	0.96%	4.12%	0.57%	40.03%	9.39%	0.7677
		SCANS	10.19%	12.98%	0.57%	36.01%	8.84%	0.7621			SCANS	0.58%	2.29%	0.00%	70.96%	20.99%	0.5147
		Modified	0.58%	7.63%	1.15%	18.73%	11.60%	0.8841			Modified	0.96%	3.82%	0.00%	40.71%	8.29%	0.7651
Phi-4	15B	Original	0.19%	3.97%	0.00%	72.71%	17.13%	0.5007	14B	14B	Original	0.19%	4.43%	0.57%	40.33%	7.18%	0.7683
		AlphaSteer+	0.00%	3.97%	0.00%	72.63%	15.47%	0.5039			AlphaSteer+	5.96%	22.44%	3.45%	13.65%	6.63%	0.8743
		AlphaSteer	0.00%	3.36%	0.00%	75.97%	16.57%	0.4704			AlphaSteer	0.77%	12.21%	0.57%	20.09%	5.52%	0.8719
		Steer	0.00%	2.29%	0.00%	84.23%	20.99%	0.3762			Steer	0.00%	0.31%	0.57%	72.33%	20.99%	0.5052
		SCANS	1.35%	5.95%	0.00%	67.78%	11.60%	0.5490			SCANS	29.04%	26.11%	9.20%	35.94%	25.41%	0.6955
		Modified	0.77%	3.82%	0.00%	53.37%	11.60%	0.6727			Modified	4.81%	3.05%	0.00%	51.86%	11.05%	0.6801